ADVANCED MATERIALS

Supporting Information

for *Adv. Mater.*, DOI 10.1002/adma.202305567

How Photogenerated I_2 Induces I-Rich Phase Formation in Lead Mixed Halide Perovskites

Yang Zhou, Simone C. W. van Laar, Daniele Meggiolaro*, Luca Gregori, Samuele Martani, Jia-Yong Heng, Kunal Datta, Jesús Jiménez-López, Feng Wang, E Laine Wong, Isabella Poli, Antonella Treglia, Daniele Cortecchia, Mirko Prato, Libor Kobera, Feng Gao, Ni Zhao, René A. J. Janssen, Filippo De Angelis and Annamaria Petrozza**

Supporting Information

How Photogenerated I_2 Induces I-rich Phase Formation in Lead Mixed Halide Perovskites

Yang Zhou[*a], *Simone C. W. van Laar*[b], Daniele Meggiolaro[g*], Luca Gregori[g,h], *Samuele Martani*[a], *Jia-Yong Heng*[c], *Kunal Datta*[b], *Jesús Jiménez-López*[a], *Feng Wang*[d], *E Laine Wong*[a], *Isabella Poli*[a], *Antonella Treglia*[a], *Daniele Cortecchia*[a], *Mirko Prato*[e], *Libor Kobera*[f], *Feng Gao*[d], *Ni Zhao*[c], *René A. J. Janssen*[b], Filippo De Angelis[g,h,i] *and Annamaria Petrozza**[a]

[a.] Center for Nano Science and Technology@Polimi, Istituto Italiano di Tecnologia, via Rubattino 81, 20134 Milano, Italy.

Email: yang.zhou@iit.it, annamaria.petrozza@iit.it, daniele.meggiolaro@cnr.it

[b.] Molecular Materials and Nanosystems, Institute for Complex Molecular Systems, Eindhoven University of Technology, P.O. Box 513, 5600 MB Eindhoven, The Netherlands.

[c.] Electronic Engineering Department, The Chinese University of Hong Kong, Shatin, N.T., Hong Kong.

[d.] Department of Physics, Chemistry and Biology, Linköping University, Linköping, Sweden

[e.] Materials Characterization Facility, Istituto Italiano di Tecnologia, Genova, Italy

[f.] Institute of Macromolecular Chemistry, Czech Academy of Sciences, Czech Republic

[g]*Computational Laboratory for Hybrid/Organic Photovoltaics (CLHYO), Istituto CNR di Scienze e Tecnologie Chimiche "'Giulio Natta"' (CNR-SCITEC), Via Elce di Sotto 8, 06123 Perugia, Italy.*

[h]*Department of Chemistry, Biology and Biotechnology, University of Perugia and INSTM, Via Elce di Sotto 8, 06123, Perugia, Italy.*

[i]*SKKU Institute of Energy Science and Technology (SIEST) Sungkyunkwan University, Suwon, Korea 440-746.*

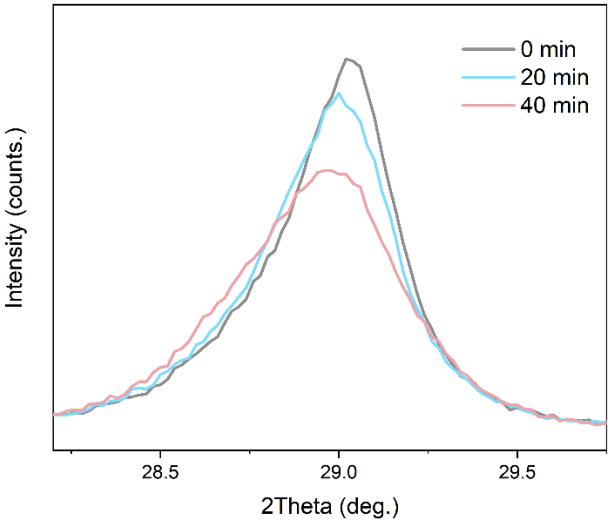

Figure S1. Shift of the (002) XRD peak of the $Cs_{0.17}FA_{0.83}PbI_{1.5}Br_{1.5}$ perovskite thin film upon I_2 exposure in the dark over 20 and 40 min.

Table S1. Estimation of variation of iodide ratio in the perovskite lattice upon I_2 exposure

Exposure time	(002) peak position	Lattice constant (Å)	Iodide ratio	Iodide ratio variation
0	29.02°	6.152	0.5	0
20 min	29.00°	6.156	0.5008	0.008
40 min	28.97°	6.162	0.5018	0.018

The relationship between the (002) peak position and the iodide ratio y (y=1-x, x is the bromide ratio) in $Cs_{0.17}FA_{0.83}Pb(I_{1-x}Br_x)_3$ perovskites has been reported[1]. Therefore, based on the shift in the (002) peak position and the relationship between (002) peak position and the iodide ratio, we can estimate the iodide ratio is increased by 0.008 and 0.018 upon I_2 exposure in the dark for 20 and 40 min, respectively.

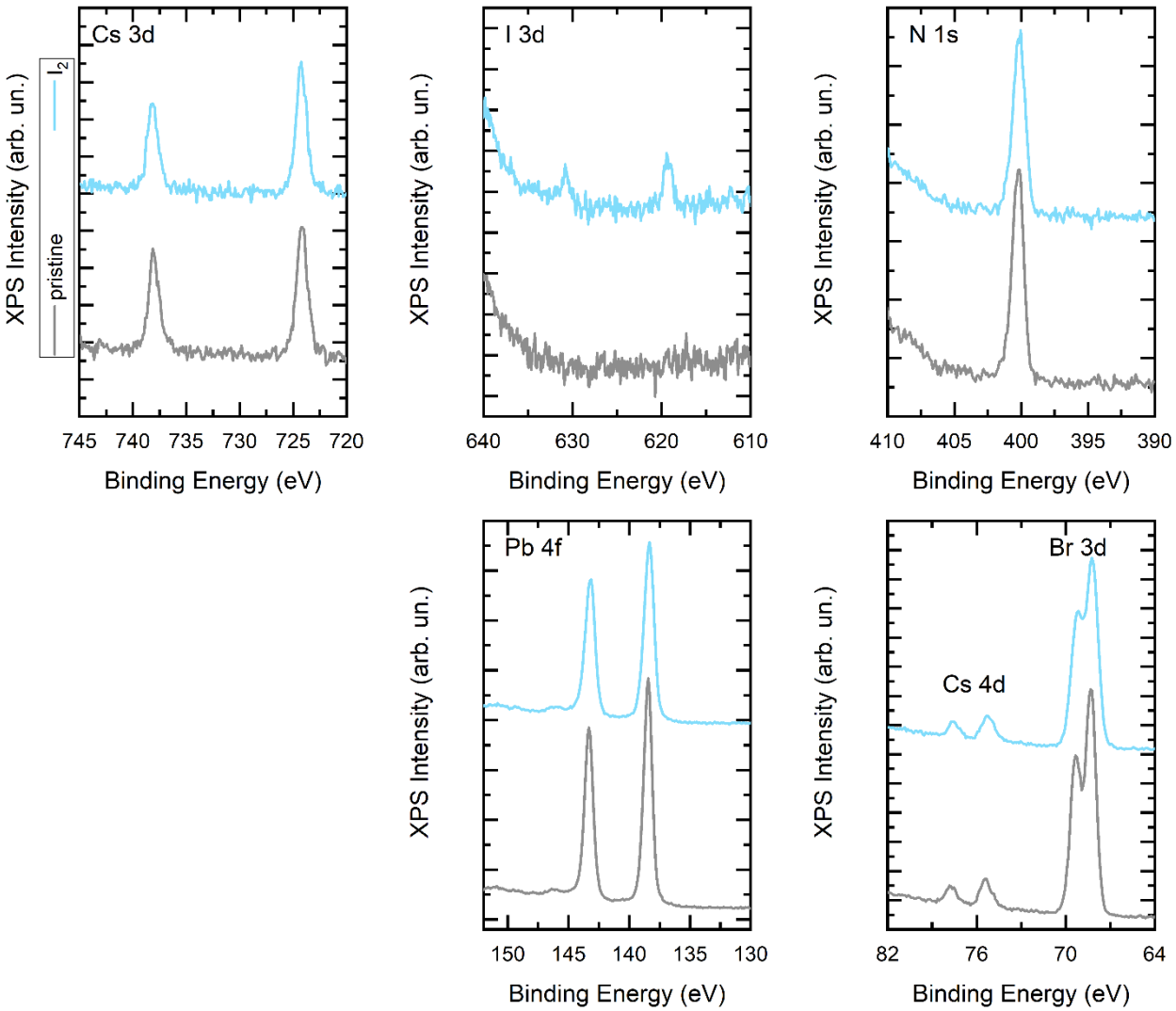

Figure S2. XPS spectra of Cs 3d, I 3d, N 1s, Pb 4f, Cs 4d and Br 3d of the $Cs_{0.17}FA_{0.83}PbBr_3$ perovskite before and after I_2 vapor exposure.

Table S2. XPS peak positions of Cs $3d_{5/2}$, N 1s, Pb $4f_{7/2}$, Br $3d_{5/2}$, Cs $4d_{5/2}$ and I $3d_{5/2}$ before and after I_2 treatment in $Cs_{0.17}FA_{0.83}PbBr_3$ perovskite

	Pure bromide perovskite	After I_2 treatment	Variation
Cs $3d_{5/2}$	724.17 eV	724.23 eV	+0.06 eV
N 1s	400.24 eV	400.15 eV	−0.09 eV
Pb $4f_{7/2}$	138.46 eV	138.36 eV	−0.10 eV
Br $3d_{5/2}$	68.30 eV	68.15 eV	−0.15 eV
Cs $4d_{5/2}$	75.38 eV	75.22 eV	−0.16 eV
I $3d_{5/2}$	NA	619 eV	NA

Table S3. Surface composition of Cs, N, Pb, Br and I derived from XPS spectra.

	Cs at%	N at %	Pb at%	Br at%	I at%
Pristine	2.4	31.1	18.2	48.4	0
After I_2 exposure	2.4	29.7	18.5	49	0.3

The possibility of forming I^- through Br^- oxidation by I_2

We first considered I^- formation through possible Br^- oxidation by I_2:

$$2Br^- + I_{2\,(g)} \rightarrow Br_{2\,(g)} + 2I^- \qquad \text{Equation S1}$$

The oxidation potentials of I_2 and Br_2 is 0.54 V and 1.07 V, respectively. According to Nernst equation, the rate constant of the reaction can be calculated:

$$K = e^{\frac{nF\Delta E}{RT}} = 1.16 \times 10^{-18} = \frac{[Br_2]}{[I_2]}$$

Where the n is the number of electrons transferred in the reaction which is 2 in this case. *F* is the Faraday constant (96485 C/mol), and ΔE is oxidation potential difference between I_2 and Br_2 which is −0.53 V. R is the ideal gas constant which is 8.31 J/(K·mol). *T* is the temperature which in our case is 298 K.

We can then estimate the concentration of I_2 in the vial. The volume of the vial is 20 mL. The vial bottom is kept at 50 °C and the vial top (sample side) is at 25 °C. Due to the temperature gradient in the vial, we use the pressure of I_2 at 50 °C of 0.29 kPa[2] to estimate the upper limit of I_2 quantity involved in the reaction. The quantify of I_2 can be calculated:

$$n(I_2) = \frac{PV}{RT} = 2.21 \times 10^{-6} mol$$

The quantity of formed Br_2 can be calculated if we assume reaction following Equation S1 can happen:

$$n(Br_2) = n(I_2) \times K = \mathbf{2.55 \times 10^{-24} mol}$$

The quantity of formed I^- following Equation S1 (if the reaction can happen) is:

$$n_1(I^-) = \mathbf{5.10 \times 10^{-24} mol}$$

Considering the XPS detection depth (t) is about 10 nm, the quantify of Br^- within this thickness of perovskite is:

$$n(Br^-) = \frac{3t \cdot A \cdot \rho}{M} = \mathbf{5.0 \times 10^{-8} mol}$$

Here A is the area exposed to I_2 vapor, which in our case is about 1.5×1.5 cm^2. ρ is the perovskite density which we take the density of $FAPbBr_3$ 3.79 g/cm^3 as an approximation. M is the mole weight mass of $Cs_{0.17}FA_{0.83}PbBr_3$ which is 507 g/mol.

According to the XPS results (Table S3), the I^- to Br^- ratio in the $Cs_{0.17}FA_{0.83}PbBr_3$ perovskite treated with I_2 is 0.3:49, therefore the actual I^- quantity should be:

$$n_2(I^-) = \mathbf{3.1 \times 10^{-10} mol}$$

The actual quantity of I^- $n_2(I^-)$ is about 13 orders of magnitude higher than $n_1(I^-)$ estimated by assuming reaction following Equation S1 can happen. Therefore, the formation of I^- when the $Cs_{0.17}FA_{0.83}PbBr_3$ perovskite exposed to I_2 is not likely to follow the route shown in Equation S1.

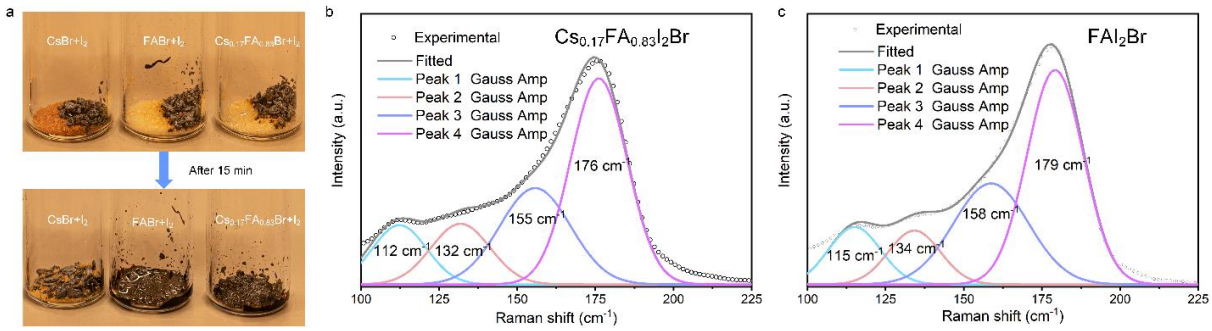

Figure S3. (a) The feasibility of I_2Br^- formation in a pure Cs, a pure FA and a mixed Cs-FA environment by mixing FABr, CsBr, and I_2 in a molar ratio of 1 : 0 : 1, 0 : 1 : 1 and 0.17 : 0.83 : 1 at an ambient temperature of 25 °C, respectively. Raman spectra of (b) $Cs_{0.17}FA_{0.83}Br$-I_2 and (c) FABr-I_2 mixtures, indicating the formation of I_2Br^- in both cases.

We checked the feasibility of I_2Br^- formation in a pure Cs, a pure FA and a mixed Cs-FA environment by mixing FABr, CsBr, and I_2 in a molar ratio of 1 : 0 : 1, 0 : 1 : 1 and 0.17 : 0.83 : 1 at an ambient temperature of 25 °C, respectively. It is shown that in the two environments containing FA, the mixtures of bromide salts and I_2 show prominent reaction to form dark red compound, while no visible reaction can be observed in the pure-Cs environment (Fig. S3a). Polyhalides typically yield intense Raman signals due to the large polarizability of their electron-rich structures; thus, we exploited this technique to probe their formation. The Raman spectrum of the compound formed in the FA-containing environments matches that of the I_2Br^- ion(Figs. S3b-c)[3], suggesting its formation in this scenario. With the existence of Cs^+, the formation of I_2Br^- ion is suppressed and is possibly due to higher charge density (smaller radius) of Cs^+ than FA^+ (Fig. S3a), which binds Br^- more tightly and increases the negative charge localization near the cation, and thus weakens the capability of Br^- to polarize I_2 to form the triple halide ion.[4]

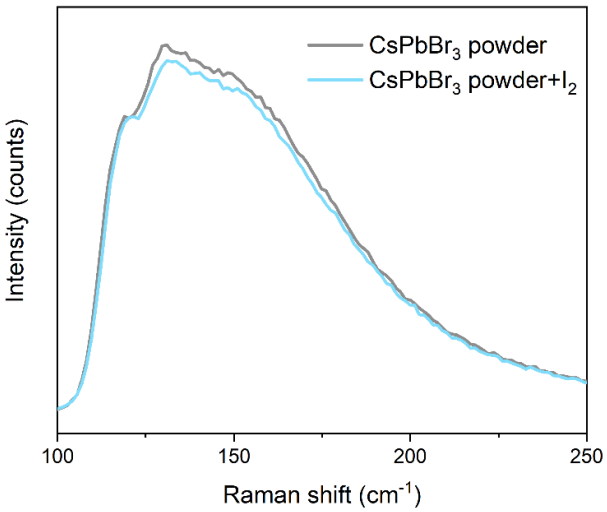

Figure S4. Raman spectrum of $CsPbBr_3$ powder and $CsPbBr_3$-I_2 mixture after mixing for 2 h.

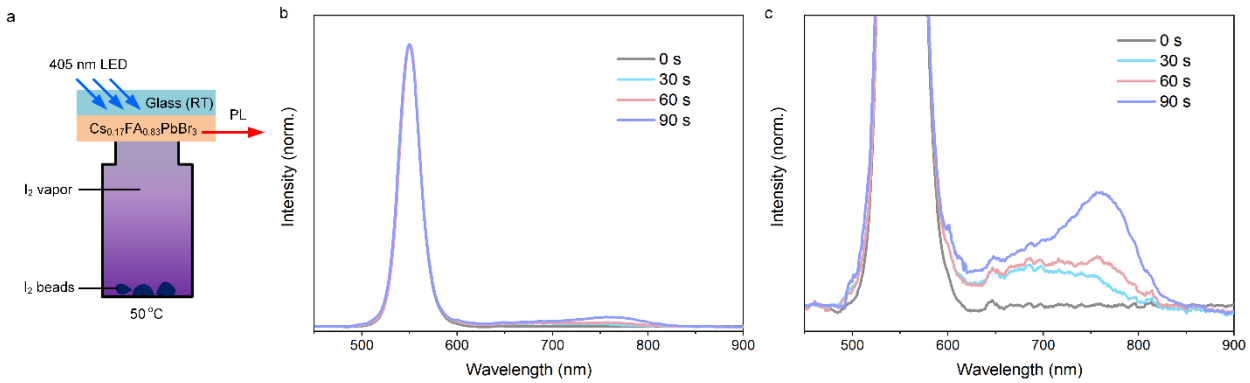

Figure S5. (a) Schematic of I_2 exposure on the $Cs_{0.17}FA_{0.83}PbBr_3$ perovskite thin film under illumination. (b) PL evolution of the $Cs_{0.17}FA_{0.83}PbBr_3$ perovskite thin film upon I_2 exposure under illumination. (c) PL redshift of the I-rich phase formed in $Cs_{0.17}FA_{0.83}PbBr_3$ perovskite thin film upon I_2 exposure under illumination.

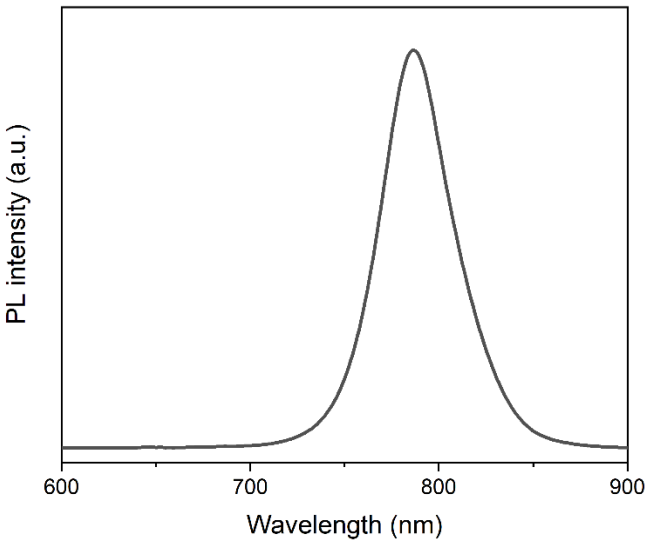

Figure S6. PL spectrum of the $Cs_{0.17}FA_{0.83}PbI_3$ pure iodide perovskite.

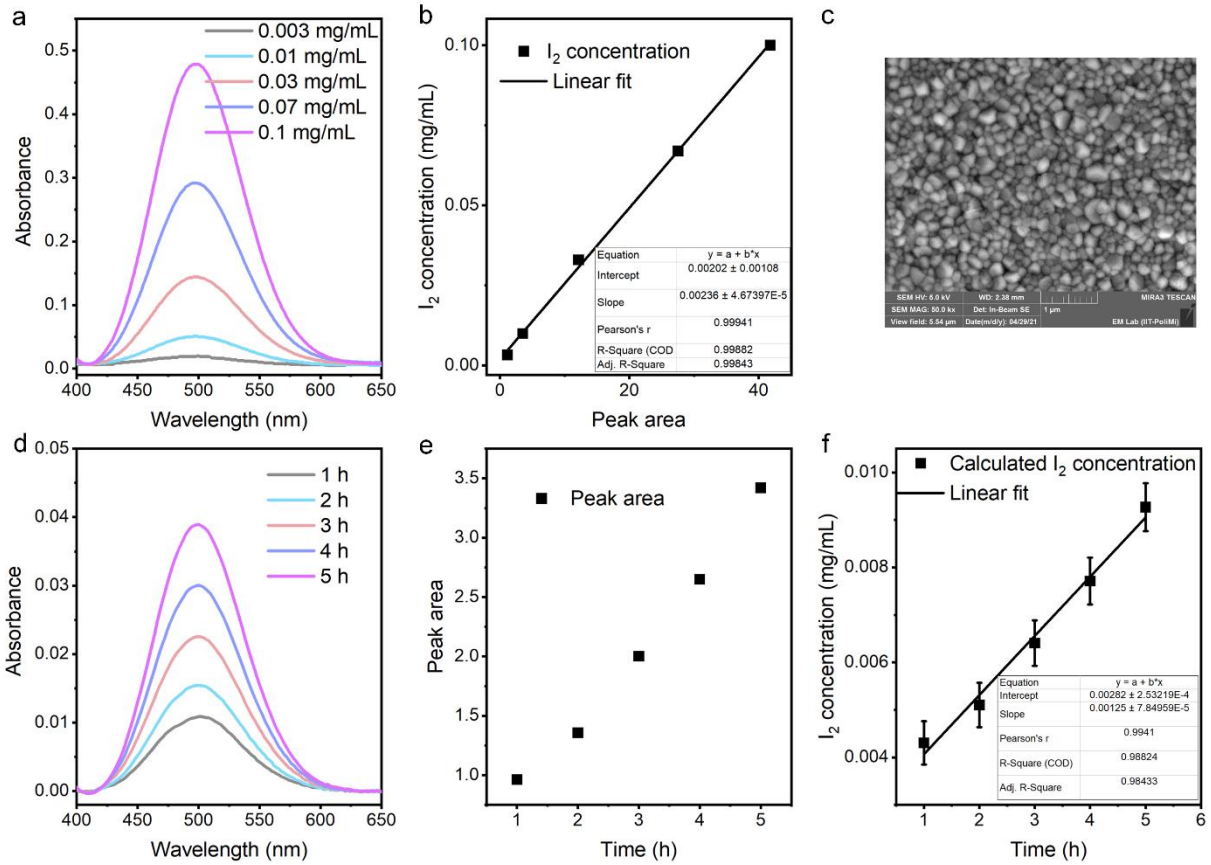

Figure S7. (a) UV-vis absorption spectra of I_2 with varied concentration in toluene. The background is removed. (b) Linear fit of t the relationship between I_2 concentration in toluene and the area of the absorption peak of I_2. (c) Scanning electron microscopy (SEM) image of the $Cs_{0.17}FA_{0.83}PbI_{1.5}Br_{1.5}$ perovskite. (d) Evolution of the UV-vis absorption of the toluene that hold the $Cs_{0.17}FA_{0.83}PbI_{1.5}Br_{1.5}$ perovskite under 1 sun illumination over 5 hours. The I_2 signal increases over time and indicates its formation. (e) The relationship between area of I_2 absorption peak and aging time of the perovskite. (d) The linear fit of the I_2 formation trend over 5 hours. The slope gives the I_2 formation rate in the toluene.

Estimation of building-up rate of I_2 vapor pressure in the grain boundaries

Under illumination, I_2 is firstly formed in the mixed I-Br perovskite, which can then be expulsed to the grain boundaries due the relief of lattice strain[5], and induce I-rich phase formation there. Indeed, halide segregation is evidenced to initiate at the grain boundaries [6]. Considering the grain boundaries are relatively closed space, the formation of I_2 can possibly vaporize there and reach a certain pressure. By preparing several I_2 solutions with known concentrations in toluene and checking their absorptions, we can get the relationship between I_2 concentration and the absorption peak area as shown in Figs. S7a-b. We checked the formation of I_2 by soaking the $Cs_{0.17}FA_{0.83}PbI_{1.5}Br_{1.5}$ perovskite thin film in anhydrous toluene and under 1 sun illumination. The area of I_2 absorption peak is used to represent the quantity of I_2 detected in toluene (Figs. S7d-e). Based on this relationship, we can know (and this will be an underestimation)how much I_2 is formed after light exposure in toluene for some time. We further did the linear fitting on the I_2 formation trend over 5 hours with the data that has been shown in Figs. S7d-e, to determine an average value of I_2 formation rate. The fitting results is shown in Figure S7f. Based on this fitting we know that the building up rate of I_2 concentration is 1.25×10^{-3} mg/(mL·h). Since the sample is hold in 6 ml toluene, the I_2 formation rate is 7.5×10^{-3} mg/h. The I_2 formation rate $r_n(I_2)$ in mole per second is:

$$r_n(I_2) = \frac{7.5 \times 10^{-3} mg}{254 \frac{mg}{mol} \times 3600 s} = 8.20 \times 10^{-9} mol/s$$

Further we estimated the volume of the space at the grain boundaries of the $Cs_{0.17}FA_{0.83}PbI_{1.5}Br_{1.5}$ perovskite. Based on the scanning electron microscopy (SEM) image shown in Fig. S7c, we estimate the average grain area to be about 0.031 μm^2. Considering the substrate we used for I_2 formation is 1.4×1.4 cm^2 in dimension, the total number of grains N_{GB} is about:

$$N_{GB} = \frac{1.4 \times 1.4 \times 10^8}{0.031} = 6.32 \times 10^{10}$$

The film thickness is about 300 nm, and the width of the grain boundaries is about 5 nm according to the SEM image (Fig. S7c). Assuming the grains have the square shape, the average dimension of the grain is 180 × 180 nm^2. Based on these we can estimate the total space volume (V_{GB}) at the grain boundaries:

$$V_{GB} = 180 \times 300 \times 2.5 \times 4 \times N_{GB} \times 10^{-27} m^3 = 3.41 \times 10^{-13} m^3$$

Therefore, the pressure building up rate P(I_2) at the grain boundary can be estimated as following:

$$P(\mathrm{I_2}) = \frac{r_n(I_2) \cdot \mathrm{R} \cdot T}{V_{GB}} = \frac{8.20 \times 10^{-9} \times 8.314 \times 297}{3.41 \times 10^{-13}} \frac{Pa}{s} = 6.4\ Pa/s$$

Here R is the gas constant of 8.314 J·mol^{-1}·K^{-1}, T is the ambient temperature (25 ^{o}C) of conducting the I_2 formation experiment. The vapor press of solid I_2 at a temperature of 25 ^{o}C is 27 Pa[2], which can be built up within tens of seconds in the grain boundaries of the perovskite under illumination. Such timescale accords well with that of halide segregation which happens within minutes under light illumination.

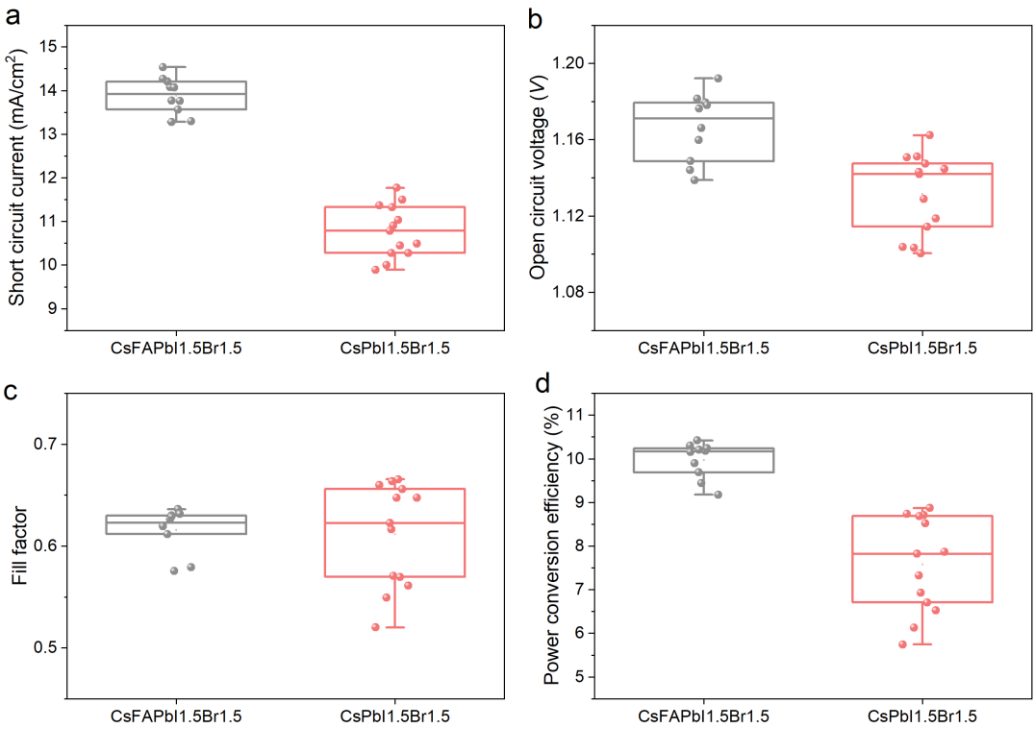

Figure S8. Statistics of photovoltaic parameters of the solar cells for in-situ PL measurement at open-circuit condition with a device structure of FTO/SnO_2/perovskite/Spiro-OMeTAD/Au. (a) Short-circuit current (J_{SC}), (b) open-circuit voltage (V_{OC}), (c) fill factor (FF) and (d) power conversion efficiency (PCE) of the solar cells prepared from the $Cs_{0.17}FA_{0.83}PbI_{1.5}Br_{1.5}$ and $CsPbI_{1.5}Br_{1.5}$ perovskites.

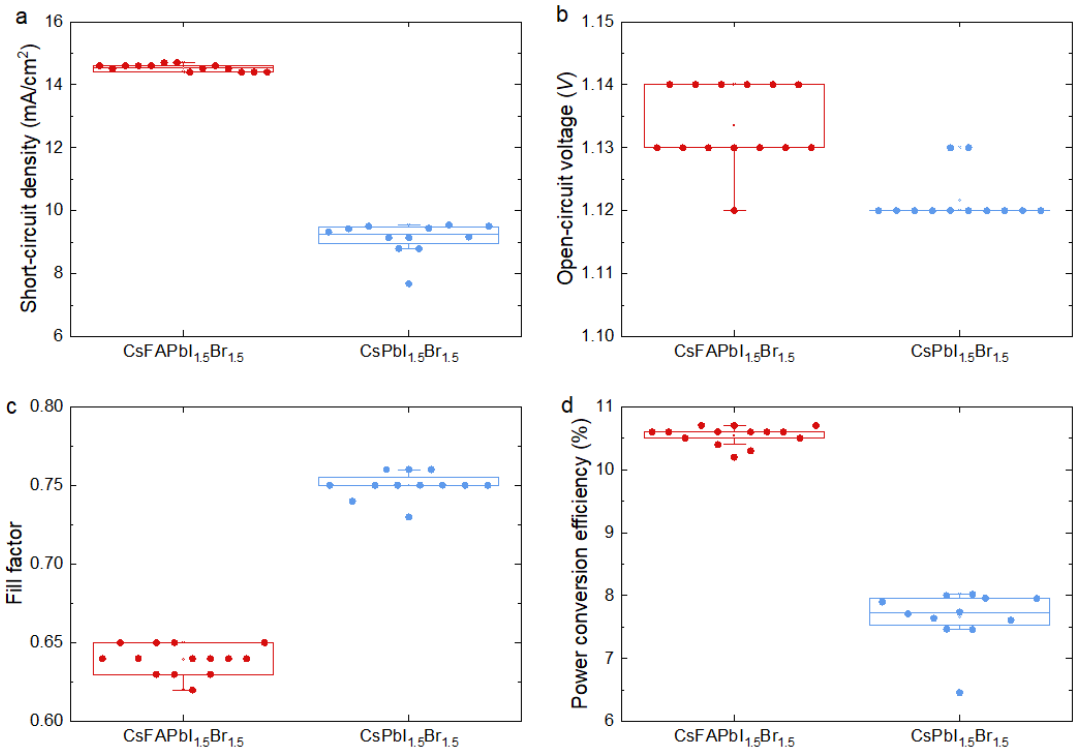

Figure S9. Statistics of photovoltaic parameters of the solar cells for in-situ PL measurement at a bias voltage of 0.8 × V_{MPP} with a device structure of ITO/SnO_2/PCBA/perovskite/Spiro-OMeTAD/MoO_3/Au. (a) Short-circuit current (J_{SC}), (b) open-circuit voltage (V_{OC}), (c) fill factor (FF) and (d) power conversion efficiency (PCE) of the solar cells prepared from the $Cs_{0.17}FA_{0.83}PbI_{1.5}Br_{1.5}$ and $CsPbI_{1.5}Br_{1.5}$ perovskites.

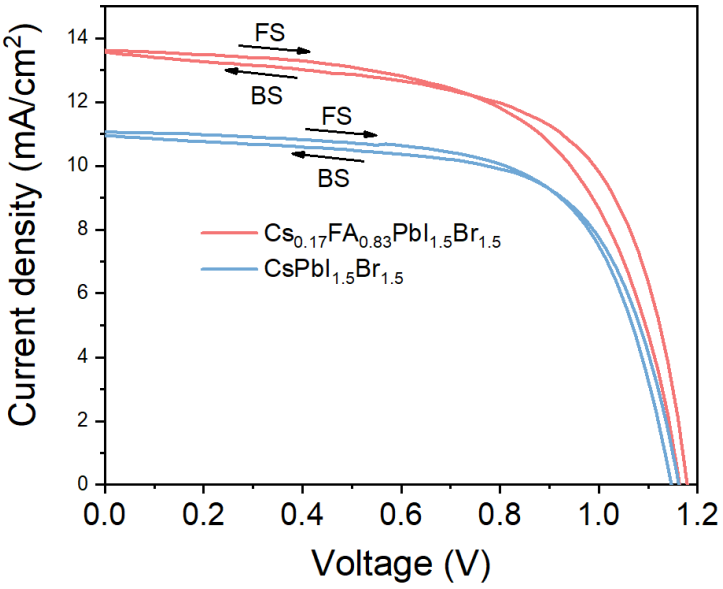

Figure S10. Current density-voltage curves of the solar cells prepared from the $Cs_{0.17}FA_{0.83}PbI_{1.5}Br_{1.5}$ and $CsPbI_{1.5}Br_{1.5}$ perovskites with a device structure of FTO/SnO_2/perovskite/Spiro-OMeTAD/Au.

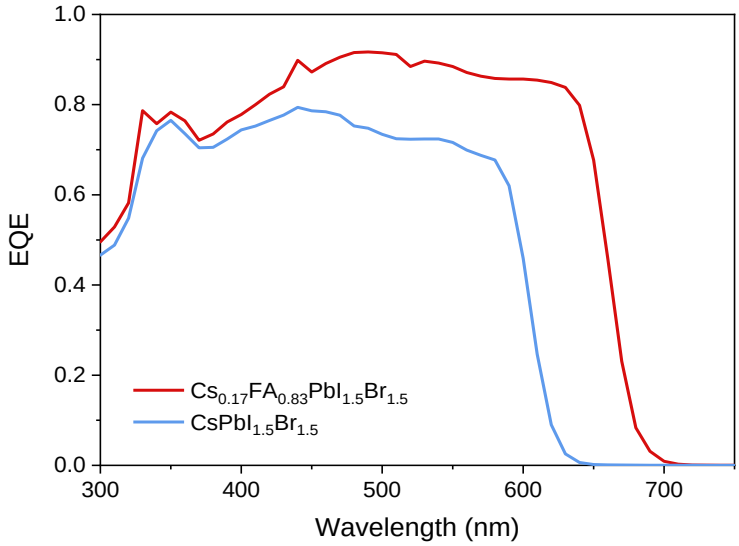

Figure S11. External quantum efficiency spectra of the solar cells with a device structure of ITO/SnO_2/PCBA/perovskite/Spiro-OMeTAD/MoO_3/Au prepared from the $Cs_{0.17}FA_{0.83}PbI_{1.5}Br_{1.5}$ and $CsPbI_{1.5}Br_{1.5}$ perovskites.

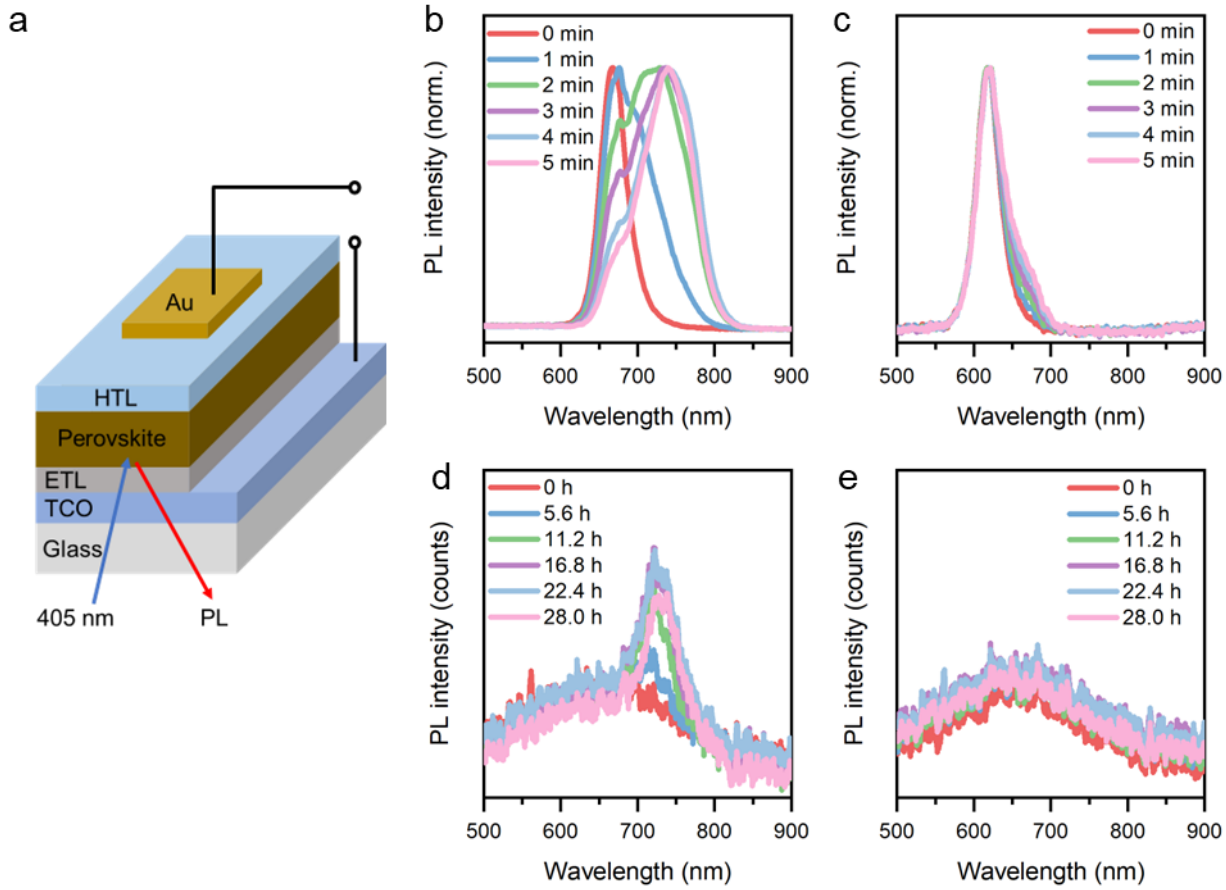

Figure S12. (a) Schematic of in-situ PL measurement of $Cs_{0.17}FA_{0.83}PbI_{1.5}Br_{1.5}$ and $CsPbI_{1.5}Br_{1.5}$ perovskite solar cells. TCO is transparent conductive oxide, ETL is electron transporting layer and HTL is hole transporting layer. PL spectra of (b) $Cs_{0.17}FA_{0.83}PbI_{1.5}Br_{1.5}$ and (c) $CsPbI_{1.5}Br_{1.5}$ perovskite solar cell under open-circuit condition and continuous illumination (λ_{ex} = 405 nm, 50 mW/cm^2) over 5 min. PL spectra of (d) $Cs_{0.17}FA_{0.83}PbI_{1.5}Br_{1.5}$ and (e) $CsPbI_{1.5}Br_{1.5}$ perovskite solar cells at a voltage bias of 0.80 times the maximum power point voltage (0.8 × V_{MPP}) and continuous illumination (λ_{ex} = 405 nm, 50 mW/cm^2) over about 28 hours.

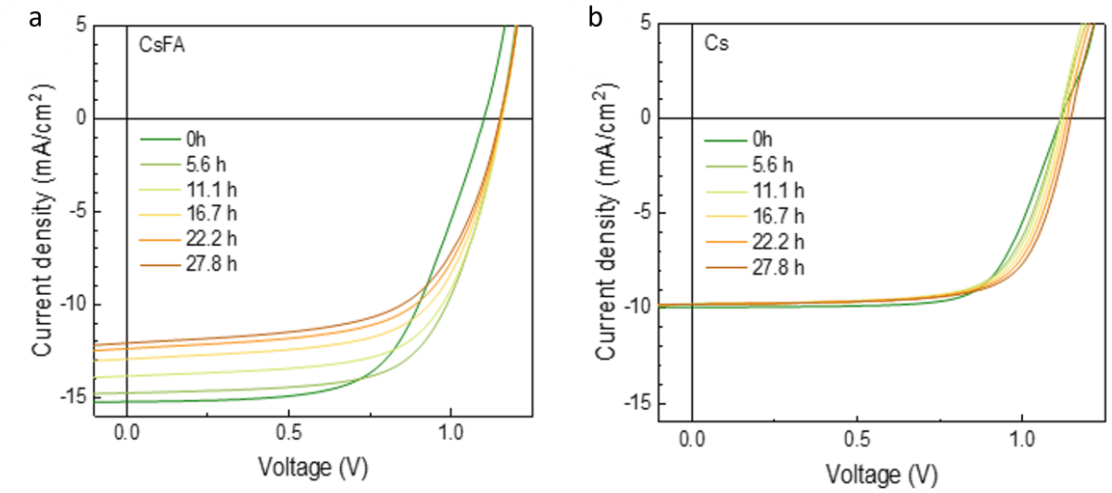

Figure S13. Current density versus voltage curves of (a) $Cs_{0.17}FA_{0.83}PbI_{1.5}Br_{1.5}$ and (b) $CsPbI_{1.5}Br_{1.5}$ *n-i-p* perovskite solar cells during in-situ PL measurement under continuous illumination (λ_{ex} = 405 nm, 50 mW/cm^2) for about 28 hours and at a voltage bias of 0.80 × V_{MPP}. These *J-V* curves are obtained in the reverse scans.

Impact of Cs^+ on the photostability of the perovskites incorporated in the solar cells

We fabricated $Cs_{0.17}FA_{0.83}PbI_{1.5}Br_{1.5}$ and $CsPbI_{1.5}Br_{1.5}$ perovskite solar cells in an *n-i-p* device architecture (Fig. S12a). The in-situ PL measurements are conducted when devices are aged either under open-circuit condition or at a voltage bias of 0.80 times the maximum power point voltage (0.80 × V_{MPP}) to check for stability under representative operating conditions. Figs. S12b-c show the evolutions of PL of $Cs_{0.17}FA_{0.83}PbI_{1.5}Br_{1.5}$ and $CsPbI_{1.5}Br_{1.5}$ perovskite solar cells under open-circuit condition with the excitation of a 405 nm light source (50 mW/cm^2). At open-circuit condition, charges are accumulated within the devices and thus we expect it to be a critical condition for bandgap stability. In fact, in $Cs_{0.17}FA_{0.83}PbI_{1.5}Br_{1.5}$ based devices (Fig. S12b) halide segregation is completed in less than 5 min, while in $CsPbI_{1.5}Br_{1.5}$ based devices in such time window the emission is suppressed (Fig. 12c). In contrast, when both types of solar cells are biased at a voltage of 0.80 × V_{MPP}, the evolutions of PL spectra become slower since charges are quickly extracted (Figs. S12d-e). Nevertheless, it is also shown that the PL emission of $Cs_{0.17}FA_{0.83}PbI_{1.5}Br_{1.5}$ based devices is not stable (Fig. S12d) while that of the $CsPbI_{1.5}Br_{1.5}$ perovskite barely changes over a time span of 167 min (Fig. 12e). During the in-situ PL measurement, the *J-V* curves of the solar cells were also simultaneously recorded. The photovoltaic performance of the $Cs_{0.17}FA_{0.83}PbI_{1.5}Br_{1.5}$ perovskite solar cells show faster reduction than those of the $CsPbI_{1.5}Br_{1.5}$ counterpart (Fig. S13)which is in agreement with earlier research[7].

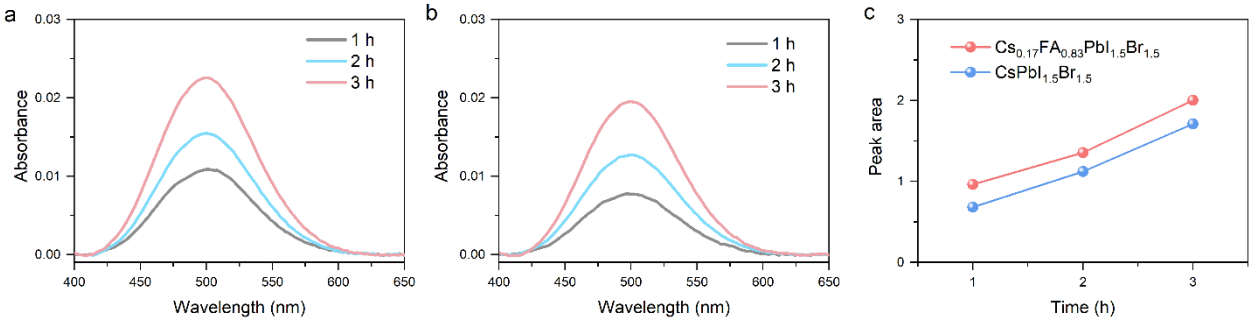

Figure S14. Evolution of I_2 signal detected by UV-visible absorption spectroscopy in anhydrous toluene holding (a) $Cs_{0.17}FA_{0.83}PbI_{1.5}Br_{1.5}$ perovskite and (b) $CsPbI_{1.5}Br_{1.5}$ perovskite over 3 h. (c) evolutions of the area of the I_2 absorption peak over 3 h for both $Cs_{0.17}FA_{0.83}PbI_{1.5}Br_{1.5}$ and $CsPbI_{1.5}Br_{1.5}$ perovskites. The background of the all absorption spectra has been removed.

We checked the I_2 formation in $Cs_{0.17}FA_{0.83}PbI_{1.5}Br_{1.5}$ and $CsPbI_{1.5}Br_{1.5}$ perovskites, by holding them separately in anhydrous toluene under a white LED exposure with intensity calibrated to 1 sun at 30 °C. The evolution of I_2 formation is monitored by checking the UV-Vis absorption of the anhydrous toluene that has been in contact with the perovskite films under light soaking. Despite Cs^+ hampering the formation of the I-rich phase, both perovskites show identical tendencies of I_2 formation through the aging process (Figs. S14a-c).

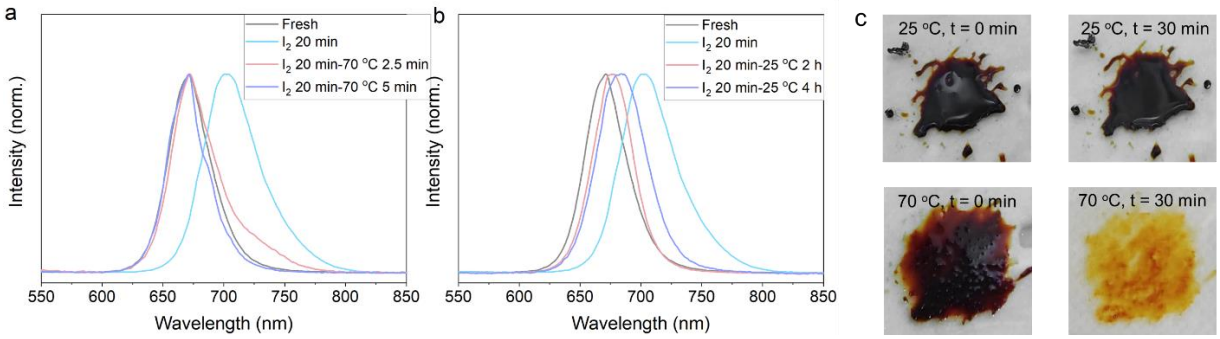

Figure S15. (a) PL emissions of the fresh $Cs_{0.17}FA_{0.83}PbI_{1.5}Br_{1.5}$ perovskite thin film, the thin film after 20 min I_2 exposure, and the thin film after 20 min I_2 exposure and then transferred to a N_2 (I_2-free) environment for storage at 25 °C. (b) PL emissions of the fresh $Cs_{0.17}FA_{0.83}PbI_{1.5}Br_{1.5}$ perovskite thin film, the thin film after 20 min I_2 exposure, and the thin film after 20 min I_2 exposure and then transferred to a N_2 (I_2-free) environment for heating at 70 °C for 2.5 and 5 min. (c) Photo images of the triple halide compound of FAI_2Br after being kept at 25 °C and 70 °C for 0 min and 30 min.

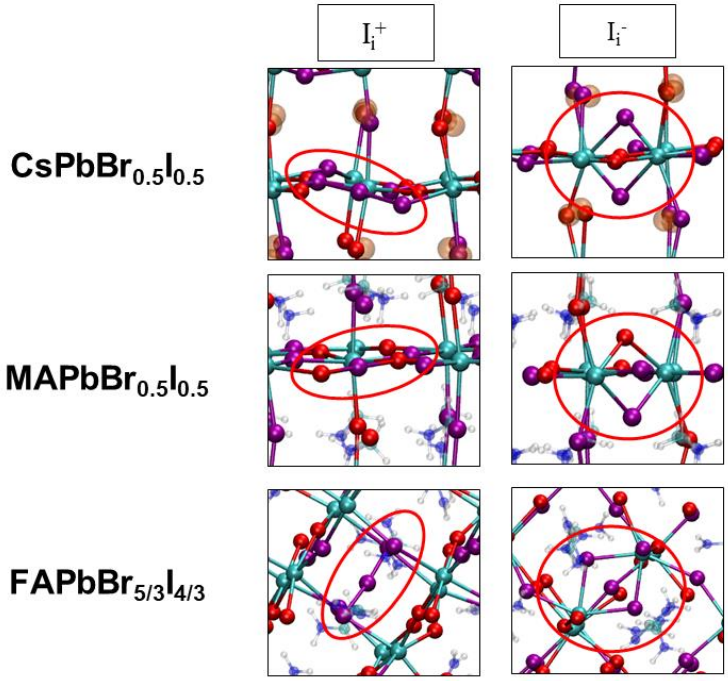

Figure S16. Structures of positive and negative iodine interstitials in the examined mixed Br/I perovskites.

References

[1] D. P. McMeekin, G. Sadoughi, W. Rehman, G. E. Eperon, M. Saliba, M. T. Hörantner, A. Haghighirad, N. Sakai, L. Korte, B. Rech, M. B. Johnston, L. M. Herz, H. J. Snaith, *Science* **2016**, 351, 151.

[2] H. H. Yolcu, *Journal of the Turkish Chemical Society, Section C: Chemical Education* **2016**, 1.

[3] A. Van den Bossche, E. De Witte, W. Dehaen, K. Binnemans, *Green Chemistry* **2018**, 20, 3327.

[4] L. E. Topol, *Inorganic Chemistry* **1968**, 7, 451.

[5] a)S. G. Motti, D. Meggiolaro, A. J. Barker, E. Mosconi, C. A. R. Perini, J. M. Ball, M. Gandini, M. Kim, F. De Angelis, A. Petrozza, *Nature Photonics* **2019**, 13, 532; b)D. Meggiolaro, S. G. Motti, E. Mosconi, A. J. Barker, J. Ball, C. Andrea Riccardo Perini, F. Deschler, A. Petrozza, F. De Angelis, *Energy & Environmental Science* **2018**, 11, 702.

[6] a)X. Tang, M. van den Berg, E. Gu, A. Horneber, G. J. Matt, A. Osvet, A. J. Meixner, D. Zhang, C. J. Brabec, *Nano Letters* **2018**, 18, 2172; b)C. G. Bischak, C. L. Hetherington, H. Wu, S. Aloni, D. F. Ogletree, D. T. Limmer, N. S. Ginsberg, *Nano Letters* **2017**, 17, 1028.

[7] a)A. J. Knight, J. B. Patel, H. J. Snaith, M. B. Johnston, L. M. Herz, *Advanced Energy Materials* **2020**, 10, 1903488; b)K. Datta, B. T. van Gorkom, Z. Chen, M. J. Dyson, T. P. A. van der Pol, S. C. J. Meskers, S. Tao, P. A. Bobbert, M. M. Wienk, R. A. J. Janssen, *ACS Applied Energy Materials* **2021**, 4, 6650.